Fibroblast Activation Protein–Targeted PET/CT with ^{68}Ga-FAPI for Imaging IgG4-Related Disease: Comparison to ^{18}F-FDG PET/CT

Yaping Luo[1,2], Qingqing Pan[1,2], Huaxia Yang[3], Linyi Peng[3], Wen Zhang[3], and Fang Li[1,2]

[1]*Department of Nuclear Medicine, Chinese Academy of Medical Sciences and Peking Union Medical College Hospital, Beijing, China;* [2]*Beijing Key Laboratory of Molecular Targeted Diagnosis and Therapy in Nuclear Medicine, Beijing, China; and* [3]*Department of Rheumatology, Chinese Academy of Medical Sciences and Peking Union Medical College Hospital, Beijing, China*

IgG4-related disease (RD) is characterized by lymphoplasmacytic infiltration enriched in IgG4-positive plasma cells and variable degrees of fibrosis with a characteristic storiform pattern. Since fibrosis is an important feature of IgG4-RD, we performed a prospective cohort study to evaluate the performance of ^{68}Ga-fibroblast activation protein inhibitor (FAPI), a recently introduced PET agent targeting fibroblast activation protein, in IgG4-RD. **Methods:** Twenty-six patients with IgG4-RD were recruited. All patients underwent both ^{68}Ga-FAPI and ^{18}F-FDG PET/CT. The positive rates of the PET/CT scans in the involved organs and the uptake values were compared. **Results:** In a total of 136 involved organs in the 26 patients, ^{68}Ga-FAPI PET/CT additionally detected 18 (13.2%) involved organs in 13 (50.0%) patients, compared with ^{18}F-FDG PET/CT. ^{68}Ga-FAPI PET/CT had a higher positive rate than ^{18}F-FDG PET/CT in detecting involvement in the pancreas, bile duct/liver, and lacrimal gland. ^{68}Ga-FAPI also demonstrated significantly higher uptake than ^{18}F-FDG in the matched disease in the pancreas, bile duct/liver, and salivary gland ($P < 0.01$). However, lymph node involvement with flip-flop uptake of ^{18}F-FDG did not accumulate ^{68}Ga-FAPI. **Conclusion:** ^{68}Ga-FAPI might be a promising imaging agent for the assessment of IgG4-RD.

Key Words: IgG4-related disease; fibroblast activation protein; ^{68}Ga-FAPI; PET/CT

J Nucl Med 2021; 62:266–271
DOI: 10.2967/jnumed.120.244723

IgG4-related disease (RD) is an autoimmune-mediated disorder associated with a diffuse mass-forming inflammatory reaction. It can affect nearly any anatomic site and may be confused with malignancy, infection, or other immune-mediated disease (*1,2*). Although IgG4-RD could affect any organ, there are predilections for certain involved organs with a synchronous or metachronous pattern, including salivary gland, orbits and lacrimal gland, pancreas, biliary tree, lung, kidney, aorta and retroperitoneum, and thyroid gland (*1–3*). The diagnosis of IgG4-RD often requires the integration of clinical, serologic, radiologic, pathologic, and immunohistologic features (*3*). The 3 central histopathologic features of IgG4-RD are lymphoplasmacytic infiltration enriched in IgG4-positive plasma cells, obliterative phlebitis, and storiform fibrosis (*4–6*). Sometimes even with supporting histopathologic evidence, clinicopathologic correlation is needed to confirm the diagnosis of IgG4-RD, and imaging is an important aspect of the diagnostic workup.

^{18}F-FDG PET can help to detect the extent of organ involvement and to monitor disease activity after treatment in IgG4-RD (*1*). In a retrospective study on ^{18}F-FDG PET/CT for differential diagnosis of patients with clinically suspected IgG4-RD, ^{18}F-FDG PET/CT had a sensitivity of 85.7% and specificity of 66.1% for diagnosing IgG4-RD, based mainly on the SUV_{max} of the major involved organ, the SUV_{max} of the submandibular glands, and the presence of multiorgan involvement (*7*). However, consistent with the false-negative results of ^{18}F-FDG PET noted in some studies (*7,8*), we also encountered cases of IgG4-RD that displayed only mild or normal ^{18}F-FDG uptake in the involved organs in our clinical practice. In the above-mentioned retrospective study, the ^{18}F-FDG uptake in the major involved organs displayed a mean SUV_{max} of 4.6 ± 1.7, with a relatively wide range from 1.1 to 7.8 (*7*). The low-grade ^{18}F-FDG uptake in these cases may partly limit the utility of ^{18}F-FDG PET in differential diagnosis, staging, and evaluation of treatment response in IgG4-RD.

Recently, ^{68}Ga-fibroblast activation protein inhibitor (FAPI), which targets fibroblast activation protein (FAP), was introduced in tumor imaging, as FAP is highly expressed in cancer-associated fibroblasts in the stroma of several tumor entities (*9,10*). In addition to solid tumors, FAP was also shown to be expressed in rheumatoid arthritis, atherosclerotic plaques, fibrosis, and ischemic heart tissue after myocardial infarction (*9,10*). Preclinical studies of immuno-PET and immuno-SPECT with radiolabeled anti-FAP antibody showed high tracer accumulation in the inflamed joints that correlated with the severity of the inflammation in murine experimental rheumatoid arthritis (*11–13*). In IgG4-RD, fibrosis arising from the extracellular matrix component produced by the large number of fibroblasts is a major histopathologic feature (*1,6*); thus, we speculate that it is possible for IgG4-RD to be imaged with ^{68}Ga-FAPI. We recently reported 2 cases of IgG4-RD showing intense ^{68}Ga-FAPI uptake in the involved organs (*14,15*). In the present study, we aimed to further evaluate the performance of ^{68}Ga-FAPI PET/CT in IgG4-RD and to compare it with the performance of ^{18}F-FDG PET/CT, which served as a reference.

Received Mar. 9, 2020; revision accepted May 19, 2020.
For correspondence or reprints contact: Fang Li, Department of Nuclear Medicine, Peking Union Medical College Hospital, Shuaifuyuan 1# Wangfujing, Dongcheng District, Beijing 100730, P.R. China.
E-mail: lifang@pumch.cn
Published online Jun. 8, 2020.

MATERIALS AND METHODS

Study Design and Patients

This is a preliminary report of an ongoing prospective study evaluating the role of ^{68}Ga-FAPI PET/CT in the management of IgG4-RD. The study was approved by the institutional review board of Peking Union Medical College Hospital (protocol ZS-1810) and registered at clinicaltrials.gov (NCT 04125511). In total, 26 patients diagnosed with IgG4-RD in the Department of Rheumatology of the Peking Union Medical College Hospital were consecutively recruited from February 2019 to January 2020. Written informed consent was obtained from each patient. All recruited patients fulfilled the 2019 American College of Rheumatology/European League Against Rheumatism classification criteria for IgG4-RD (*3*). After enrollment, patients were referred for ^{18}F-FDG and ^{68}Ga-FAPI PET/CT for evaluation of the disease, and these two imaging studies were performed within 1 wk after enrollment. The imaging characteristics were analyzed afterward.

PET/CT Imaging

The ^{68}Ga-FAPI was radiolabeled manually immediately before injection. Briefly, to adjust the pH to 3.5–4.0, 92 μL of sodium acetate (1.25 M) were added to 1 mL of $^{68}GaCl_3$ eluent ($^{68}Ga^{3+}$ in 1.0 M HCl) obtained from a ^{68}Ge/^{68}Ga generator (ITG). After the addition of an aliquot of 20 μL (1 μg/μL) of FAPI-04 (CA94025; CSBio Co.), the mixture was heated to 100°C for 10 min. The reaction solution was diluted to 5 mL and passed through a preconditioned Sep-Pak C18 Plus Light cartridge (Waters), and the cartridge was eluted with 0.5 mL of 75% ethanol to obtain the final product. The radiochemical purity of the product was analyzed by thin-layer chromatography. The ^{68}Ga-FAPI injections were filtered through a 0.22-μm Millex-LG filter (EMD Millipore) before clinical use.

^{18}F-FDG was synthesized in-house with an 11-MeV cyclotron (CTI RDS 111; Siemens).

The PET scans were performed on dedicated PET/CT scanners (Biograph 64 TruePoint TrueV [Siemens] or Polestar m660 [SinoUnion]). Two patients underwent ^{18}F-FDG PET/CT at outside hospitals. For ^{18}F-FDG PET/CT, the patients fasted for over 6 h, and the blood glucose levels were monitored (4.5–8.8 mmol/L) before an injection of ^{18}F-FDG (5.55 MBq/kg). The PET/CT images (2 min/bed position) were acquired with an uptake time of 68.5 ± 12.1 min (range, 47–90 min). For ^{68}Ga-FAPI PET/CT, imaging was performed (2–3 min/bed position) with an uptake time of 54.4 ± 15.8 min (range, 40–80 min) after an injection of 85.2 ± 27.0 MBq (range, 55.5–162.8 MBq) of ^{68}Ga-FAPI. The emission scan was obtained from the tip of the skull to the mid thigh. All patients underwent unenhanced low-dose CT (120 kV, 30–50 mAs) for attenuation correction and anatomic reference. The acquired data were reconstructed using ordered-subset expectation maximization (Siemens Biograph 64: 2 iterations, 8 subsets, gaussian filter of 5 mm in full width at half maximum, 168 × 168 image size; SinoUnion Polestar: 2 iterations, 10 subsets, gaussian filter of 4 mm in full width at half maximum, 192 × 192 image size).

Image Interpretation and Statistical Analysis

The PET/CT images were transferred to a Siemens multimodality workplace (Syngo). Two experienced nuclear medicine physicians visually assessed the PET/CT images and were in consensus for the image interpretation of involved organs. The presence and sites of IgG4-RD involvement and the intensity of the uptake in the lesions were recorded. Increased radioactivity compared with the background uptake was defined as being positive. The SUVs of the lesions were measured by the same nuclear medicine physician using the volume-of-interest method with a unified standard. The McNemar test was used to statistically compare the positive rates of ^{68}Ga-FAPI and ^{18}F-FDG PET/CT in detecting organs involving IgG4-RD. The differences in SUV_{max} between ^{68}Ga-FAPI and ^{18}F-FDG PET/CT were tested using a paired Student *t* test. A *P* value of less than 0.05 was considered statistically significant.

RESULTS

Clinical Characteristics

Twenty-six patients with IgG4-RD (20 men and 6 women; mean ± age SD, 51.5 ± 12.9 y; range, 17–64 y) were enrolled in the present study. Nineteen patients had newly diagnosed IgG4-RD that was treatment-naïve; 7 patients had a previous history of IgG4-RD and had been treated with prednisone or other medication but had recurrent or persistent disease at enrollment. The median level of serum IgG4 was 14,500 mg/L (range, 355–73,400 mg/L; normal limits, 80–1,400 mg/L). Seventeen patients (65.4%) underwent biopsy for diagnosis of IgG4-RD (biopsy sites: pancreas [n = 7], salivary gland [n = 4], lacrimal gland [n = 2], lymph node [n = 2], lung [n = 2], retroperitoneal mass [n = 1], kidney [n = 1], and gallbladder [n = 1]).

In the recruited patients, IgG4-RD most commonly involved the pancreas (19/26, 73.1%), salivary gland (19/26, 73.1% [submandibular gland, 19/26, 73.1%; parotid gland, 7/26, 26.9%; sublingual gland, 7/26, 26.9%]), lymph nodes (16/26, 61.5%), and lacrimal gland (14/26, 53.8%; extraocular muscle was also involved in 1 patient). Other involved organs included lung (9/26, 34.6%), pleura (6/26, 23.1%), bile duct/liver (6/26, 23.1%; gallbladder was also involved in 1 patient), retroperitoneal fibrosis or periaortitis (7/26, 26.9%), kidney (5/26, 19.2%), prostate (9/26, 34.6%), seminal vesicle (3/26, 11.5%), peritoneum (3/26, 11.5%), nasal cavity (3/26, 11.5%), and pituitary stalk (1/26, 3.8%). The clinical characteristics are summarized in Table 1.

Comparison of ^{68}Ga-FAPI and ^{18}F-FDG PET/CT

^{68}Ga-FAPI PET/CT was visually positive for detecting involvement of IgG4-RD in all patients, whereas ^{18}F-FDG PET/CT results were positive in 24 (92.3%) of the 26 patients. In the 136 involved organs in the 26 patients, ^{68}Ga-FAPI PET/CT additionally detected 18 (13.2%) involved organs in 13 (50.0%) patients, compared with ^{18}F-FDG PET/CT (^{68}Ga-FAPI–positive/^{18}F-FDG–negative), including the disease in the pancreas (8/19), lacrimal gland (4/14), sublingual gland (2/7), submandibular gland (1/19), bile duct/liver (2/6), and nasal cavity (1/3). However, all lymph node involvement that was ^{18}F-FDG–avid was missed by ^{68}Ga-FAPI PET/CT (^{68}Ga-FAPI–negative/^{18}F-FDG–positive). False-negative organ involvement with both tracers (^{68}Ga-FAPI–negative/^{18}F-FDG–negative) was found in 2 patients. The first of these patients (patient 12) had IgG4-related lung disease that had been previously treated with prednisone for 3 y. The lung disease did not show ^{18}F-FDG or ^{68}Ga-FAPI uptake on PET (^{68}Ga-FAPI–negative/^{18}F-FDG–negative), but some patches in the lung were shown in the coregistered CT scan. The second of these patients (patient 19) had membranous glomerulonephritis and was negative for the kidney disease on both ^{18}F-FDG and ^{68}Ga-FAPI PET/CT. The remaining involvement was interpreted as being positive with both tracers (^{68}Ga-FAPI–positive/^{18}F-FDG–positive). The detection rate of ^{68}Ga-FAPI and ^{18}F-FDG PET/CT for IgG4-RD involvement is shown in Table 2. The diagnostic performance of dual-tracer PET/CT in each case is shown in Supplemental Table 1 (supplemental materials are available at http://jnm.snmjournals.org).

When we visually compared the uptake and the extension of involved organs detected on PET/CT, ^{68}Ga-FAPI showed much

TABLE 1
Clinical Characteristics and IgG4-RD Involvement

Patient No.	Age	Sex	Biopsy site	Treatment	Serum IgG4 (mg/L)	Involvement of IgG4-RD
1	21	M	Pancreas	Prednisone, MMF	29,300	Pituitary stalk, lacrimal gland, salivary gland, lung, pleura, pericardium, liver, gallbladder, pancreas, prostate, LN
2	58	M	Parotid	None	11,300	Salivary gland, lung, pancreas, prostate, LN
3	52	M	Gallbladder	None	71,700	Lacrimal gland, salivary gland, intrahepatic bile duct, pancreas, prostate, LN
4	56	M	Lacrimal gland	Prednisone	14,600	Lacrimal gland, extraocular muscle, salivary gland, pleura, pancreas, periaortitis, peritoneum, LN
5	60	M	None	None	14,400	Lacrimal gland, salivary gland, pancreas
6	59	F	Pancreas	None	11,700	Lacrimal gland, salivary gland, pancreas, LN
7	24	F	None	None	3,510	Retroperitoneal fibrosis
8	55	M	Pancreas	None	34,100	Lacrimal gland, salivary gland, intrahepatic bile duct, liver, pancreas, prostate, LN
9	62	M	Lacrimal gland	None	27,900	Lacrimal gland, salivary gland, nasal cavity, pleura, prostate, seminal vesicle, peritoneum, LN
10	63	M	None	None	1,530	Retroperitoneal fibrosis, LN
11	17	M	Submandibular gland, pancreas	None	1,380	Salivary gland, pancreas
12	42	F	Lung	Prednisone	355	Lacrimal gland, salivary gland, lung
13	55	M	None	None	21,600	Lacrimal gland, salivary gland, lung, liver, pancreas, prostate, LN
14	57	M	None	None	33,700	Lacrimal gland, salivary gland, lung, pleura, periaortitis, pancreas, prostate, seminal vesicle, LN
15	64	M	LN, kidney	None	28,200	Nasal cavity, lung, pleura, intrahepatic bile duct, pancreas, periaortitis, kidney, prostate, LN
16	63	F	Submandibular gland, LN	None	47,200	Lacrimal gland, salivary gland, lung, pancreas, LN
17	63	M	Submandibular gland	None	73,400	Lacrimal gland, salivary gland, nasal cavity, lung, intrahepatic bile duct, pancreas, LN
18	40	M	None	None	6,710	Pancreas, kidney, LN
19	51	M	Pancreas	Prednisone	34,500	Salivary gland, pancreas, kidney
20	57	M	None	Prednisone, MMF	54,400	Lacrimal gland, salivary gland, pancreas, kidney
21	59	F	None	None	3,370	Retroperitoneal fibrosis, LN
22	55	M	None	None	3,210	Salivary gland, pancreas
23	63	M	Pancreas	None	11,900	Lacrimal gland, salivary gland, pancreas, prostate, LN
24	45	M	Pancreas	Prednisone, sirolimus, MMF	1,730	Pancreas
25	50	F	Lung	Prednisone	580	Salivary gland, lung, pleura
26	47	M	Retroperitoneal mass	None	31,100	Kidney and perirenal masses, peritoneum and retroperitoneal mass, seminal vesicle

MMF = mycophenolate mofetil; LN = lymph node.

higher contrast or detected more extensive disease in the pancreas, bile duct/liver, and salivary gland than ^{18}F-FDG did in more than 50% of the recruited patients with the above involvements. For quantitative comparison, the SUV_{max} of the matched disease in the pancreas, bile duct/liver, and salivary gland was significantly higher on ^{68}Ga-FAPI PET/CT (pancreas, 15.22 ± 8.99; bile duct/liver, 9.42 ± 4.36; salivary gland, 8.26 ± 3.90) than on ^{18}F-FDG PET/CT (pancreas, 4.19 ± 2.52; bile duct/liver, 4.58 ± 2.08; salivary gland, 4.88 ± 1.90) (paired Student t test, $P <$ 0.01). Meanwhile, the lymph node involvement had significantly higher uptake on ^{18}F-FDG PET/CT (SUV_{max}, 6.37 ± 1.72) than on ^{68}Ga-FAPI PET/CT (SUV_{max}, 1.61 ± 0.76) in all patients with IgG4-related lymphadenopathy (paired Student t test, $P <$ 0.0001). When we compared the uptake of ^{68}Ga-FAPI versus ^{18}F-FDG in involved lacrimal gland, lung/pleura, periaortitis/retroperitoneal fibrosis, kidney, and prostate/seminal vesicle, the average SUV_{max} presented no relevant differences ($P > 0.05$). The visual and quantitative comparison between ^{68}Ga-FAPI and ^{18}F-

TABLE 2
Detectability of ^{68}Ga-FAPI and ^{18}F-FDG PET/CT in IgG4-RD

Involved organ	^{68}Ga-FAPI	^{18}F-FDG	*P*
Lacrimal gland	14/14 (100%)	10/14 (71.4%)	0.125
Salivary gland	19/19 (100%)	18/19 (94.7%)	1.0
Lung/pleura	10/11 (90.9%)	10/11 (90.9%)	1.0
Pancreas	19/19 (100%)	11/19 (57.9%)	0.0078*
Bile duct/liver	6/6 (100%)	4/6 (66.7%)	0.480
Periaortitis/retroperitoneal fibrosis	7/7 (100%)	7/7 (100%)	1.0
Kidney	4/5 (80.0%)	4/5 (80.0%)	1.0
Prostate/seminal vesicle	10/10 (100%)	10/10 (100%)	1.0
Lymph node	0/16 (0%)	16/16 (100%)	<0.0001*

*Difference in positive rate between ^{68}Ga-FAPI and ^{18}F-FDG is significant.

FDG PET/CT in organs involving IgG4-RD is shown in Figure 1 and Table 3, respectively; and examples of maximum-intensity projections of the dual-tracer PET scans in IgG4-RD are shown in Figure 2.

DISCUSSION

^{68}Ga-FAPI is a recently introduced pan-tumor PET agent targeting FAP, a type II transmembrane serine protease. Overexpression of FAP protein is a distinct feature of cancer-associated fibroblasts but is not found in normal fibroblasts (*9,10*). In IgG4-RD, myofibroblasts and fibroblasts are activated by polarized CD4-positive T-cell populations to drive fibrosis (*1*). Histopathologically, fibroblasts and myofibroblasts are intermingled with lymphoplasmacytic infiltrate and fibrosis, especially in the active phase of IgG4-RD (*2*). Although there is no direct evidence to confirm the overexpression of FAP in IgG4-RD, we speculate that the high accumulation of ^{68}Ga-FAPI in IgG4-RD results from the uptake by the activated fibroblasts or myofibroblasts.

In our study, we found high ^{68}Ga-FAPI uptake in the organs involving IgG4-RD, especially in the pancreas, bile duct/liver, and salivary gland. In contrast, lymph node involvement was ^{68}Ga-FAPI–negative. There are 5 histologic patterns in IgG4-related lymphadenopathy, including multicentric Castleman diseaselike, follicular hyperplasia, interfollicular expansion, progressive transformation of germinal centerlike, and nodal inflammatory pseudotumorlike types. Fibrosis is not seen in most IgG4-related lymphadenopathy except in inflammatory pseudotumorlike lesions (*6,16*). This fact explains the false-negative results for ^{68}Ga-FAPI PET in lymph node involvement in our study. Regarding the histopathologic confirmation of IgG4-RD, the 3 major features are

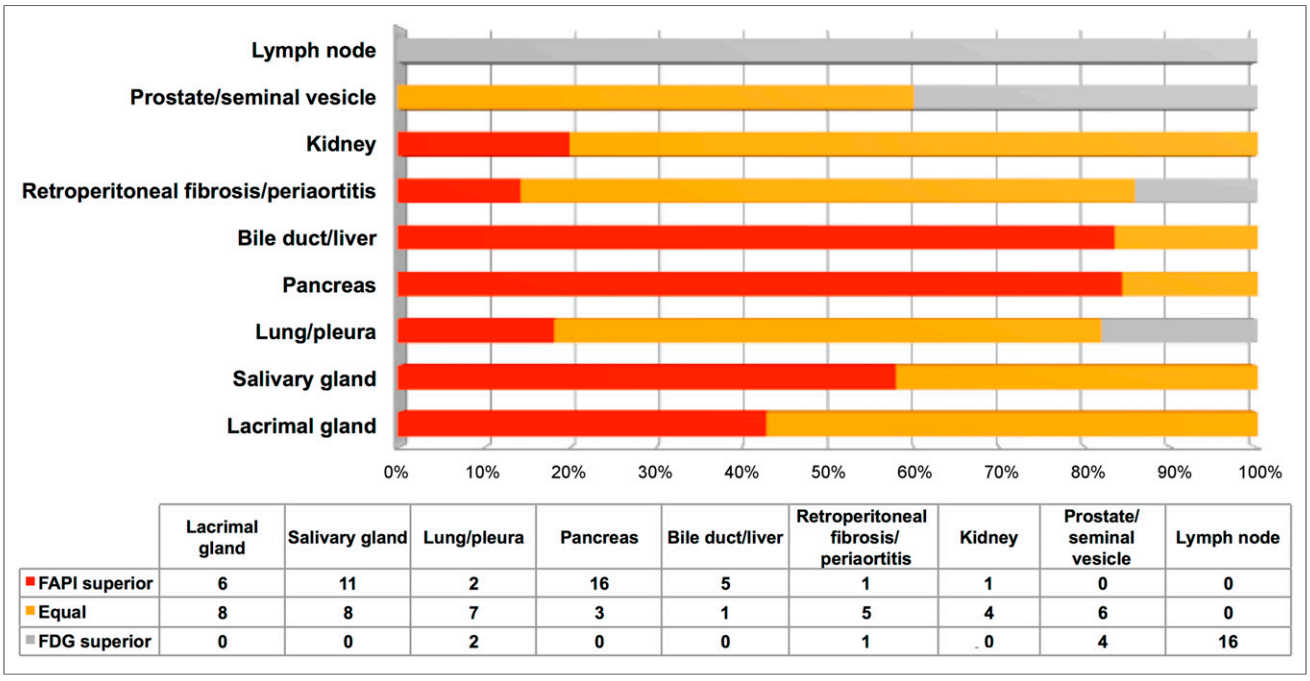

	Lacrimal gland	Salivary gland	Lung/pleura	Pancreas	Bile duct/liver	Retroperitoneal fibrosis/ periaortitis	Kidney	Prostate/ seminal vesicle	Lymph node
FAPI superior	6	11	2	16	5	1	1	0	0
Equal	8	8	7	3	1	5	4	6	0
FDG superior	0	0	2	0	0	1	0	4	16

FIGURE 1. Visual comparison of ^{68}Ga-FAPI and ^{18}F-FDG PET/CT in organs involving IgG4-RD.

TABLE 3
SUV_{max} of IgG4-RD Involvement in ^{68}Ga-FAPI and ^{18}F-FDG PET/CT

Involved organ	^{68}Ga-FAPI	^{18}F-FDG	*P*
Lacrimal gland	4.81 ± 1.64	5.64 ± 4.10	0.433
Salivary gland	8.26 ± 3.90	4.88 ± 1.90	0.0008*
Lung/pleura	6.69 ± 7.21	4.33 ± 2.56	0.196
Pancreas	15.22 ± 8.99	4.19 ± 2.52	<0.0001*
Bile duct/liver	9.42 ± 4.36	4.58 ± 2.08	0.0081*
Periaortitis/retroperitoneal fibrosis	8.71 ± 4.04	6.11 ± 2.45	0.157
Kidney	9.44 ± 6.67	4.02 ± 1.58	0.106
Prostate/seminal vesicle	6.38 ± 2.16	7.30 ± 2.90	0.450
Lymph node	1.61 ± 0.76	6.37 ± 1.72	<0.0001*

*Difference of SUV_{max} between ^{68}Ga-FAPI and ^{18}F-FDG is significant.

dense lymphoplasmacytic infiltration, storiform fibrosis, and obliterative phlebitis. Infiltration of IgG4-positive plasma cells may also be found in other diseases (e.g., antineutrophil cytoplasmic autoantibody–associated disease, diabetic nephropathy, multicentric Castleman disease, rheumatoid arthritis, and pancreatic cancers); the characteristic storiform fibrosis and obliterative phlebitis are considered to be more specific findings in IgG4-RD, and fibrosis is a histologic prerequisite for the diagnosis (*6*). On this account, the histopathologic diagnosis of IgG4-RD through lymph node biopsy alone is difficult because fibrosis and obliterative phlebitis are lacking (*1,3*). Unlike ^{18}F-FDG, which accumulates in cancer cells and active inflammatory lesions from an enhancement of glycolytic flux, the ^{68}Ga-FAPI uptake is suggested to be associated with the degree of fibrosis; thus, ^{68}Ga-FAPI PET may be preferred to ^{18}F-FDG PET in providing an optimal site for biopsy to diagnose IgG4-RD.

We found ^{68}Ga-FAPI to be superior or at least equal to ^{18}F-FDG for detecting IgG4-RD in the lacrimal gland, salivary gland, pancreas, and bile duct/liver in all recruited patients. Because mild ^{18}F-FDG uptake by the salivary glands is usually observed in PET/CT as a normal variant, and the intense uptake in extraocular muscles may sometimes mask orbital disease (*17,18*), the low background uptake of ^{68}Ga-FAPI in the head and neck (*19,20*) makes it advantageous over ^{18}F-FDG in detecting IgG4-RD in these organs. Moreover, ^{68}Ga-FAPI has a favorable dosimetry profile and tracer kinetics for PET/CT imaging (*21*).

IgG4-RD was initially recognized in the pancreas (*6*), which was also the most commonly affected organ in our study. For diagnosis with PET/CT, a diffusely enlarged pancreas with moderate to intense ^{18}F-FDG uptake without pancreaticobiliary duct obstruction is an important strong indicator of IgG4-RD (*22*). However, a focal lesion in the pancreas with patchy ^{18}F-FDG uptake is less likely to indicate IgG4-RD and did not allow differentiation from pancreatic tumors (*7*). In our study, the pancreatic disease in 2 patients was depicted as focal lesions in the head of the pancreas on ^{18}F-FDG PET/CT, but ^{68}Ga-FAPI PET/CT obviously showed diffuse pancreatic disease with intense radioactivity in these 2 individuals (Fig. 2, patients 13 and 18). This finding enhanced confidence that IgG4-RD was present when the images were interpreted. However, diffusely increased ^{68}Ga-FAPI uptake in the pancreas should also be differentiated with pancreatic cancer with tumor-induced pancreatitis (*23*). In another 8 patients, ^{68}Ga-FAPI PET/CT additionally detected pancreatic disease that was not ^{18}F-FDG–avid, thus improving the detectability of IgG4-RD in the pancreas (^{68}Ga-FAPI vs. ^{18}F-FDG, 100% vs. 57.9%, $P < 0.01$). Similarly, ^{68}Ga-FAPI PET/CT

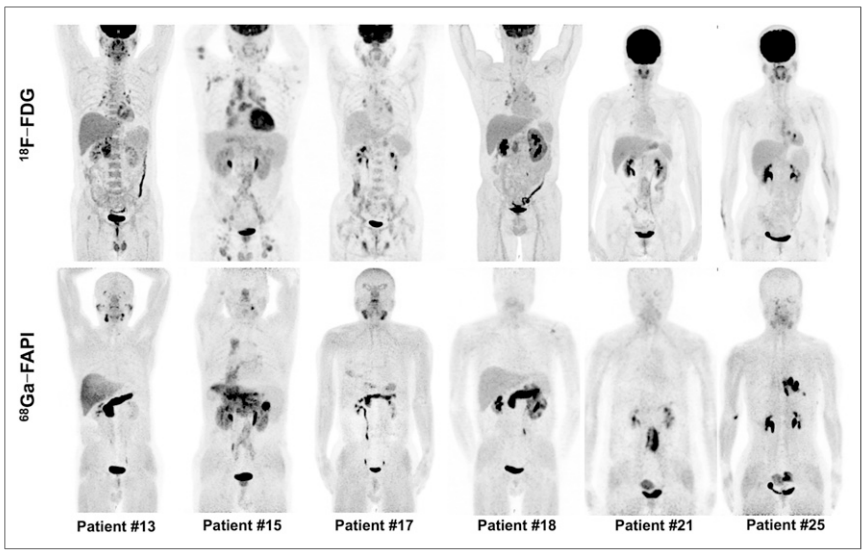

FIGURE 2. Intraindividual comparison of 6 patients with IgG4-RD undergoing ^{18}F-FDG and ^{68}Ga-FAPI PET/CT. Examples show superiority of ^{68}Ga-FAPI to ^{18}F-FDG in depicting involvement of IgG4-RD in pancreas (patients 13, 15, 17, and 18), bile duct/liver (patients 13, 15, and 17), retroperitoneal fibrosis (patient 21), lung/pleura (patient 25), and salivary gland (patients 13 and 17). Hypermetabolic lymph nodes in ^{18}F-FDG PET/CT did not show uptake of ^{68}Ga-FAPI (patients 15 and 17). Renal involvement (patients 15 and 18) was both ^{18}F-FDG–avid and ^{68}Ga-FAPI–avid. There was also unspecific ^{68}Ga-FAPI uptake in uterus (patients 21 and 25).

had a higher rate of detecting involvement of the bile duct/liver than ^{68}Ga-FAPI PET/CT did, although the difference was not statistically significant, probably because of the limited sample size (^{68}Ga-FAPI vs. ^{18}F-FDG, 100% vs. 66.7%; $P > 0.05$).

Few cases with involvement in the prostate, aorta, and lung had visually lower uptake of ^{68}Ga-FAPI than of ^{18}F-FDG at these anatomic sites. We think the cause is probably the higher positron range and inferior image quality of ^{68}Ga; thus, delineation of some small lesions (e.g., periaortitis that was smaller than 1 cm in patient 4) and prostatic disease adjacent to the bladder may be hampered by ^{68}Ga-FAPI when compared with ^{18}F-FDG. Prostate cancer also has moderate to intense uptake of ^{68}Ga-FAPI (*19,24,25*); therefore, IgG4-related prostatitis must be differentiated from prostate cancer in elderly patients.

Glucocorticoid therapy is the first-line, standard-of-care approach for most patients with IgG4-RD. A good and rapid response to glucocorticoids is a characteristic feature of IgG4-RD (*1*). The results of ^{18}F-FDG PET/CT before and after treatment correlated well with treatment response in most cases of IgG4-RD (*8,22*). As for ^{68}Ga-FAPI, we previously reported a case of IgG4-RD showing marked improvement of the lesions detected on ^{68}Ga-FAPI PET/CT at baseline after treatment with prednisone and cyclophosphamide for 2 mo (*14*). The value of ^{68}Ga-FAPI in treatment response monitoring needs to be further investigated.

Our study had several limitations. First, some recruited patients did not have histopathologic confirmation of IgG4-RD. Although biopsies are essential in many settings to establish the diagnosis of IgG4-RD and exclude mimickers, the 2019 American College of Rheumatology/European League Against Rheumatism classification criteria for IgG4-RD emphasized that biopsy is not required when the diagnosis of IgG4-RD is straightforward on the basis of clinical, serologic, and radiologic findings (*3*). Such criteria are compatible with clinical practice and essential to appropriate diagnosis for patients in both clinical and research settings. Second, immunohistochemical staining of FAP was not performed in our study. Previous studies have determined that ^{68}Ga-FAPI binds with high specificity and selectivity to FAP-positive tumor cells (*9,10*). We think the uptake of ^{68}Ga-FAPI in IgG4-RD may share the same mechanism; however, further studies are warranted. Third, the heterogeneity of PET/CT protocols (e.g., uptake time, dose, and use of 2 different PET/CT scanners and reconstruction parameters) in our study may bias the SUV measurements.

CONCLUSION

In the present study, we found that ^{68}Ga-FAPI PET/CT had a higher detection rate or higher uptake than ^{18}F-FDG did in IgG4-RD in most involved organs, especially in the pancreas, bile duct/liver, lacrimal gland, and salivary gland. However, IgG4-related lymphadenopathy was not ^{68}Ga-FAPI–avid, a finding that may be attributed to the fact that IgG4-related lymphadenopathy usually lacks the characteristic storiform fibrosis. Further studies are warranted to clarify the role of ^{68}Ga-FAPI in monitoring IgG4-RD.

DISCLOSURE

This work was supported by the CAMS Innovation Fund for Medical Sciences (CIFMS, 2017-I2 M-3-001). No other potential conflict of interest relevant to this article was reported.

KEY POINTS

QUESTION: Is ^{68}Ga-FAPI PET/CT superior to ^{18}F-FDG PET/CT in detecting organ involvement in IgG4-RD?

PERTINENT FINDINGS: In our prospective cohort study of 26 patients with IgG4-RD, ^{68}Ga-FAPI PET/CT showed a higher detection rate or higher uptake than ^{18}F-FDG did in most involved organs, except lymph nodes.

IMPLICATIONS FOR PATIENT CARE: ^{68}Ga-FAPI PET/CT might be a promising tool in the assessment of IgG4-RD.

REFERENCES

1. Kamisawa T, Zen Y, Pillai S, Stone JH. IgG4-related disease. *Lancet.* 2015; 385:1460–1471.
2. Kubo K, Yamamoto K. IgG4-related disease. *Int J Rheum Dis.* 2016;19:747–762.
3. Wallace ZS, Naden RP, Chari S, et al. The 2019 American College of Rheumatology/European League Against Rheumatism classification criteria for IgG4-related disease. *Ann Rheum Dis.* 2020;79:77–87.
4. Cheuk W, Chan JK. IgG4-related sclerosing disease: a critical appraisal of an evolving clinicopathologic entity. *Adv Anat Pathol.* 2010;17:303–332.
5. Smyrk TC. Pathological features of IgG4-related sclerosing disease. *Curr Opin Rheumatol.* 2011;23:74–79.
6. Deshpande V, Zen Y, Chan JK, et al. Consensus statement on the pathology of IgG4-related disease. *Mod Pathol.* 2012;25:1181–1192.
7. Lee J, Hyun SH, Kim S, et al. Utility of FDG PET/CT for differential diagnosis of patients clinically suspected of IgG4-related disease. *Clin Nucl Med.* 2016;41:e237–e243.
8. Ebbo M, Grados A, Guedj E, et al. Usefulness of 2-[^{18}F]-fluoro-2-deoxy-D-glucose-positron emission tomography/computed tomography for staging and evaluation of treatment response in IgG4-related disease: a retrospective multicenter study. *Arthritis Care Res (Hoboken).* 2014;66:86–96.
9. Lindner T, Loktev A, Altmann A, et al. Development of quinoline-based theranostic ligands for the targeting of fibroblast activation protein. *J Nucl Med.* 2018;59:1415–1422.
10. Loktev A, Lindner T, Mier W, et al. A tumor-imaging method targeting cancer-associated fibroblasts. *J Nucl Med.* 2018;59:1423–1429.
11. Laverman P, van der Geest T, Terry SY, et al. Immuno-PET and immuno-SPECT of rheumatoid arthritis with radiolabeled anti-fibroblast activation protein antibody correlates with severity of arthritis. *J Nucl Med.* 2015;56:778–783.
12. Terry SY, Koenders MI, Franssen GM, et al. Monitoring therapy response of experimental arthritis with radiolabeled tracers targeting fibroblasts, macrophages, or integrin $\alpha_v\beta_3$. *J Nucl Med.* 2016;57:467–472.
13. van der Geest T, Laverman P, Gerrits D, et al. Liposomal treatment of experimental arthritis can be monitored noninvasively with a radiolabeled anti-fibroblast activation protein antibody. *J Nucl Med.* 2017;58:151–155.
14. Luo Y, Pan Q, Zhang W. IgG4-related disease revealed by ^{68}Ga-FAPI and ^{18}F-FDG PET/CT. *Eur J Nucl Med Mol Imaging.* 2019;46:2625–2626.
15. Pan Q, Luo Y, Zhang W. Recurrent immunoglobulin G4-related disease shown on ^{18}F-FDG and ^{68}Ga-FAPI PET/CT. *Clin Nucl Med.* 2020;45:312–313.
16. Zen Y, Nakanuma Y. IgG4-related disease: a cross-sectional study of 114 cases. *Am J Surg Pathol.* 2010;34:1812–1819.
17. Nakamoto Y, Tatsumi M, Hammoud D, Cohade C, Osman MM, Wahl RL. Normal FDG distribution patterns in the head and neck: PET/CT evaluation. *Radiology.* 2005;234:879–885.
18. Basu S, Houseni M, Alavi A. Significance of incidental fluorodeoxyglucose uptake in the parotid glands and its impact on patient management. *Nucl Med Commun.* 2008;29:367–373.
19. Giesel FL, Kratochwil C, Lindner T, et al. ^{68}Ga-FAPI PET/CT: biodistribution and preliminary dosimetry estimate of 2 DOTA-containing FAP-targeting agents in patients with various cancers. *J Nucl Med.* 2019;60:386–392.
20. Loktev A, Lindner T, Burger EM, et al. Development of fibroblast activation protein-targeted radiotracers with improved tumor retention. *J Nucl Med.* 2019;60:1421–1429.
21. Meyer C, Dahlbom M, Lindner T, et al. Radiation dosimetry and biodistribution of ^{68}Ga-FAPI-46 PET imaging in cancer patients. *J Nucl Med.* 2020;61:1171–1177.
22. Zhang J, Chen H, Ma Y, et al. Characterizing IgG4-related disease with ^{18}F-FDG PET/CT: a prospective cohort study. *Eur J Nucl Med Mol Imaging.* 2014;41:1624–1634.
23. Luo Y, Pan Q, Zhang W, Li F. Intense FAPI uptake in inflammation may mask the tumor activity of pancreatic cancer in ^{68}Ga-FAPI PET/CT. *Clin Nucl Med.* 2020;45:310–311.
24. Kratochwil C, Flechsig P, Lindner T, et al. ^{68}Ga-FAPI PET/CT: tracer uptake in 28 different kinds of cancer. *J Nucl Med.* 2019;60:801–805.journal
25. Khreish F, Rosar F, Kratochwil C, Giesel FL, Haberkorn U, Ezziddin S. Positive FAPI-PET/CT in a metastatic castration-resistant prostate cancer patient with PSMA-negative/FDG-positive disease. *Eur J Nucl Med Mol Imaging.* 2020;47:2040–2041.journal